Auger Recombination and Charge-Carrier Thermalization in Hg_n^--Cluster Photoelectron Studies

R. Busani, R. Giniger, T. Hippler, and O. Cheshnovsky*

School of Chemistry, the Sackler Faculty of Exact Sciences, Tel-Aviv University, 69978 Israel

(Received 9 July 2002; published 24 February 2003)

Photoelectron spectra (PES) of Hg_n^- show strong dependence of spectral features on photon energy, i.e., peak tailing and band gap filling. This dependence suggests the existence of complex photoinduced processes in parallel with the direct photodetachment process. The "corrupted" PES, taken with intermediate photon energy, carry the signature of interband absorption followed by charge-carrier thermalization and Auger electron ejection in Hg_n^-. These processes, so significant in the photophysics of bulk semiconductors and nanoparticles, have not yet been identified in clusters.

DOI: 10.1103/PhysRevLett.90.083401 PACS numbers: 36.40.Wa, 33.60.–q, 36.40.Cg, 36.40.Vz

In monovalent metal clusters, such as the alkali or the coinage metals, the congestion of states develops with cluster size into a continuous density of states of half-filled bands, allowing for the evolution of the metallic state [1]. In principle, bivalent metals could be semiconductors. In the condensed phase, it is the overlap between the *s* and *p* bands, attained by the high coordination number, which enables the formation of partially filled bands and, consequently, brings about the metallic behavior. In clusters of bivalent metals, a critical size for the *s*-*p* band merging is expected. The onset of the metallic state in the bivalent mercury clusters has been the subject of numerous experimental and theoretical studies of neutral and positively charged mercury clusters [2–8]. None of those studies, however, directly probed the *s*-*p* band merging in mercury clusters.

We have recently addressed the problem of the *s*-*p* band merging in neutral mercury clusters by studying the mass-resolved photoelectron spectra (PES) of negatively charged mercury clusters, Hg_n^-. Spectra were recorded in the size range $n = 3$–280 with 7.9 [9] and 6.4 eV [10] photons. This study is based on the conjecture that the equilibrium geometry changes between the *negatively* charged cluster and the *neutral* cluster hardly effect the *s*-*p* band gap of large clusters. Our argument is that the excess electron in Hg_n^- resides in the lowest unoccupied molecular orbital of the corresponding neutral cluster. This electron can be photodetached, leaving the resulting neutral cluster in its electronic ground state. Alternatively, electrons detached from the $2n$ orbitals of the 6*s* "band" leave the resulting neutral cluster in an "electron-hole pair" excited state. Thus, the gap in the PES of the negatively charged cluster represents the excitation band gap for the corresponding neutral cluster.

With increasing cluster size, the binding energy (BE) of the excess 6*p* electron increases. The BE of the highest 6*s* state is practically constant (~ 4 eV), and the *s*-*p* band gap shrinks from 3.6 eV ($n = 3$) to 0.2 eV ($n = 250$). Extrapolation indicates *s*-*p* band closure for $\sim Hg_{400\pm50}$, a considerably larger size than those previously reported ($n = 80$–100). The electronic structure of mercury clusters in the size range of $n = 3$ to $\sim 400 \pm 50$ is that of a semiconductor cluster, with a 6*s* "valence band" and a 6*p* "conduction band." It turned out, however, that with lower detachment energies (e.g., 4.66 eV), the PES varied, showing in some cases clogged band gaps. To resolve these unexpected findings, we have systematically studied the dependence of the PES of Hg_n^- on the detachment energy.

In this Letter, we show that the detachment energy dependence of the PES suggests the existence of complex photoinduced processes, competing with photodetachment. We show that our previous conclusions [9,10] concerning the band gap in mercury clusters are valid. The corrupted PES, taken with lower photon energy, carry the signature of interband absorption followed by charge-carrier thermalization and Auger electron ejection in Hg_n^-. These processes, so significant in the photophysics of bulk semiconductors and nanoparticles, have not yet been identified in clusters.

Clusters were generated by passing 2.5 bars of argon through the heated reservoir of mercury (200–250 °C) inside a 10 Hz pulsed nozzle [11]. The expansion, intersected by a pulsed electron beam (~ 200 eV), generated a wide distribution of negatively and positively charged mercury clusters. Hg_n^- clusters were mass resolved with a coaxial time-of-flight mass spectrometer. Vacuum ultraviolet PES of the mass-resolved clusters were taken with a 0.5 mJ excimer laser (6.4 or 7.9 eV) using a "magnetic-bottle" photoelectron spectrometer (MBPES) [12,13]. For other photon energies, we have used a tunable optical parametric oscillator (OPO) system [14], coupled to a modified MBPES [15]. This new spectrometer can be switched between a high collection efficiency (60%) and a low efficiency (4%) polarization sensitive mode. Spectra were accumulated, typically with 5000 laser shots, with ~ 5 photoelectrons events per shot. The spectrometer was calibrated daily with the PES of I^- ions. Laser power was attenuated to record and analyze single-photon PES only (linear with laser power).

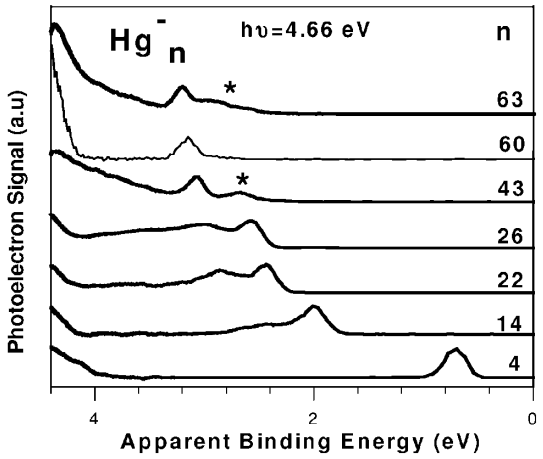

FIG. 1. Photoelectron spectra of selected Hg_n^- clusters excited with 4.66 eV photons. For comparison, note the PES of Hg_{60}^- (6.4 eV photons) showing a well-defined band gap. Stars mark two photon features.

When relevant, residual two-photon spectral features (quadratic with laser power) are indicated in the figures.

In Fig. 1 we present representative PES of Hg_n^- taken with 4.66 eV photons. In the small cluster sizes the band gaps are distinct, and the lone peaks related to the $6p$ electrons are narrow. In larger clusters, tails of the $6p$ peaks extend into the gap, clogging it at $n > 20$. For comparison, we include the PES of Hg_{60}^- taken with 6.4 eV photons, in which the gap is clearly defined and lacks any background signal.

To elucidate the nature of these gap-filled spectra, we have recorded PES of several Hg_n^- clusters, with several photon energies for each cluster size. In Fig. 2, we present four sets of PES where $n = 9, 12, 30, 40$. These spectra reveal the following characteristics: at low and at high detachment energies, the spectra exhibit a low BE peak ($6p$ electron) followed by a gap at higher BE. At intermediate detachment photon energies, the peaks are tailed towards high BE, filling the gap at larger cluster sizes (Hg_{20}, Hg_{40}). The dominant features of the spectra in Fig. 2, at all photon detachment energies, are due to single-photon absorption. We believe that the band gaps in the PES recorded at the high detachment energies reflect real gaps in the density of states in mercury clusters. We deduce that in parallel to direct photodetachment additional single-photon processes in the Hg_n^- clusters are manifested in the PES. These spectra do not necessarily project the binding energies of the electrons in the clusters. Consequently, the energy axis of Figs. 1, 2, and 4 is titled "apparent binding energy."

In Fig. 3 we schematically illustrate the photoprocesses, which give rise to the experimental findings. The two arrows on the left side of the diagram represent direct photodetachment from the $6s$ or the $6p$ states. Direct electron detachment in the negatively charged mercury cluster is expressed in a $6p$ electron peak and a wide $6s$ band separated by a band gap (black spectrum in Fig. 3).

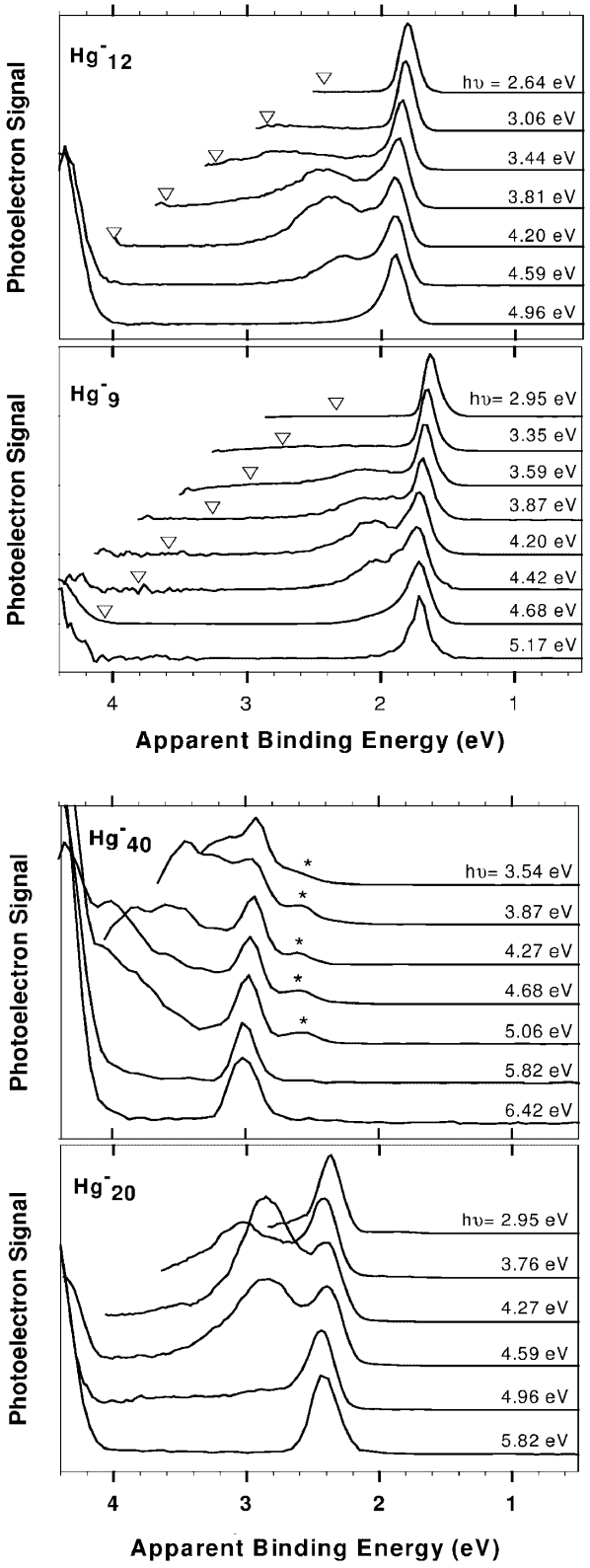

FIG. 2. PES of Hg_n^-, taken over a wide range of excitation energies. (a) The spectra of Hg_9^- and Hg_{12}^-, characterized with high BE tails, but no band gap clogging. The triangles mark the maximum extent of the tails, according to our interpretation. (b) The spectra of Hg_{20}^- and Hg_{40}^-, with completely clogged band gaps at some photon energies. Stars mark two photon features.

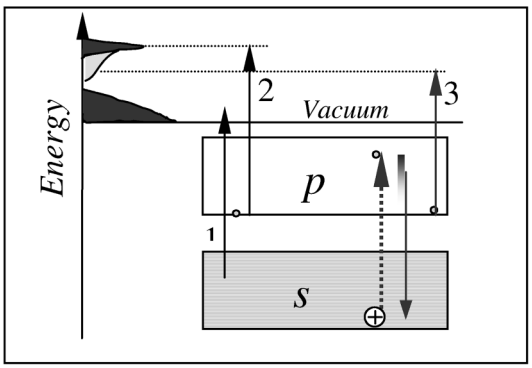

FIG. 3. Energy diagram of the processes responsible for the tailed PES. Direct photodetachment is represented by arrows 1 and 2, resulting in the electron energy distribution shown in black. Interband excitation (dotted arrow) generates an electron hole pair. Auger electron ejection, in parallel to some thermalization, ends in electron ejection of lower kinetic energy (arrow 3) building up the tails of the $6p$ peaks (tinted in gray).

In addition to photodetachment, interband absorption may occur for photon energies, $h\nu$, which exceed the band gap (BG). The excited electron-hole pair is described on the right-hand side of the diagram (dotted arrow). The photoexcited negatively charged cluster contains two electrons in the $6p$ conduction band and one hole in the $6s$ valence band. Electron-hole recombination may result in Auger electron ejection.

The kinetic energy distributions resulting from direct detachment and from the Auger process are practically identical as long as the electron and the hole do not thermalize prior to the Auger process. In the absence of thermalization, an Auger process should manifest itself in an enhanced cross section for photodetachment, as well as in the partial loss of the polarization of the PES. However, if some thermalization of the electron-hole pair occurs, the resulting Auger photoelectron spectrum shifts to lower kinetic energies (right two arrows). An obvious manifestation of this process is low kinetic energy tailing in the $6p$ peak of the PES. A long tail may lead to the filling of the s-p band gap. Note that a similar low energy tailing is expected in the $6s$ band, but, due to its width, these features are not clearly discernible.

Unlike the delayed thermionic emission phenomena, observed in the PES of some metal [16,17] and carbon [16,18] cluster anions, our tails represent dynamic *partial* thermalization in parallel to the competing Auger process. The shape of the tail is governed by the dynamics of the system and not its thermodynamics. The identification of electron emission from only partially thermalized electrons has been recently reported on Na_n^+ clusters [19] and Pt_3^- clusters [20,21].

Some observed correlations in the tailing phenomena rectify the validity of our interpretation:

(A) The interband transition and the resulting tailing occurs only if the photon energy exceeds the band gap ($h\nu > \mathrm{BG}$) and is smaller than the energy span of the bands ($h\nu < \mathrm{BG} + \Delta p + \Delta s$). Δs and Δp denote the widths of the s and p bands, respectively. In intermediate energies, the intensity of interband excitation depends on the transition probability. This condition is consistent with the fact that only intermediate photon energies exhibit the tailing phenomena.

(B) The thermalization of the electron-hole pair parallels the Auger process. Therefore, the spectra exhibit continuous tails extending from the $6p$ peaks. The extent of thermalization, however, is bound by the band gap. Consequently, the maximum apparent extent of the tail is $h\nu - \mathrm{BG}$ and depends on the excitation energy for a given cluster. In Fig. 2(a), we have marked the maximal apparent binding energies of the tail by triangles. We assume that BG in the negatively charged cluster equals BG extracted from the PES, which relates to the neutral cluster. Note that indeed the tails do not exceed our anticipated limit.

(C) When the extent of the tail $h\nu - \mathrm{BG}$ is larger than the band gap, namely, $h\nu - \mathrm{BG} > \mathrm{BG}$ or $h\nu > 2\mathrm{BG}$, the band gap may be filled by the tail. Indeed, in the PES of Hg_{20}^- and Hg_{40}^- [Fig. 2(b)] the band gap is completely filled with photoelectrons [22].

The detailed energy distributions of the tails depend on the relative rates of thermalization of the electron-hole and the Auger processes and are beyond the scope of our current discussion. The integral intensities of the tails depend on the interband transition probabilities. Preliminary results indicate peaking of the absorption cross section at photon energies of 4.2 eV. Detailed study of the excitation probability of interband transitions in these clusters will be presented elsewhere [23]. We do not exclude the possibility of plasmon enhancement of the electron-hole pair excitation.

The polarization dependence of our PES strongly supports the scenario outlined in the above discussion. In Fig. 4, we present the PES of Hg_9^- and Hg_{20}^- excited at 3.44 and 4.96 eV, respectively. The two curve pairs represent PES with the polarization of the light parallel and perpendicular to the time-of-flight tube, taken with our MBPES in the polarization sensitive mode. Note that the narrow peaks exhibit strong polarization dependence. In contrast, the tails are practically insensitive to the laser polarization. This is consistent with the notion that the tail originates from delayed processes, where polarization memory is lost. The tails in all of our PES exhibit the same insensitivity to polarization. Bordas, Broyer, and co-workers [17] have recently introduced the distinction between prompt photodetachment and delayed thermionic emission using the polarization dependence of photoelectrons. On large, we follow their approach.

The rate of Auger deexcitation in photoexcited nanoparticles is proportional to the square of the light intensity [24]. This result is well understood, since at least two excited electron-hole pairs are required for the Auger process in an initially neutral single nanoparticle. In the case of negatively charged clusters, the excess electron

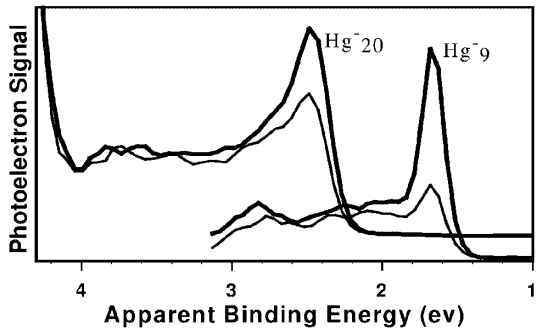

FIG. 4. The polarization dependence of the PES of Hg_9^- and Hg_{20}^- excited at 3.44 and 4.96 eV, respectively. The thick and thin lines represent parallel and perpendicular laser polarization, respectively. The sharp peaks, attributed to the direct photodetachment of the $6p$ electron, show strong polarization dependence, while the tails are insensitive to the laser polarization.

facilitates the Auger process upon the excitation of a single electron-hole pair. Because of the small dimensions of the cluster, the two electrons and the hole are closely located. This allows for an efficient Auger process, which is linear with light intensity. In the nanoparticle experiments as well as in our cluster experiments, the rate of recombination is of the same order of magnitude as the rate of charge-carrier thermalization. The identification of parallel thermalization and Auger processes in clusters is unique to the current work. As separate phenomena, there are several reports that highlight thermalization [19–21]. The recently reported indirect photodetachment via Feschbach absorption resonances in the anion cluster C_3^- [25] is similar in essence to our Auger process.

Finally, we emphasize that generally, in negatively charged clusters, the yield of Auger electron ejection might be high, due to their small size and low electron affinity. Thus, the combination of thermalization with Auger recombination might corrupt the PES, which originates from direct photodetachment. It is highly desirable to combine PES data from several excitation energies, for a meaningful interpretation of PES of anionic clusters.

This research was supported by the James Franck German–Israeli Binational Program in Laser-Matter Interaction, by the U.S.–Israel Binational Foundation, and by the Israel Science Foundation administered by the Israel Academy of Sciences.

*Electronic address: orich@chemsgl.tau.ac.il

[1] W. A. de Heer, Rev. Mod. Phys. **65**, 611 (1993); *Clusters of Atoms and Molecules I*, edited by H. Haberland (Springer-Verlag, Berlin, 1995).
[2] G. M. Pastor and K. H. Bennemann, in *Clusters of Atoms and Molecules I* (Ref. [1]), pp. 86–113.
[3] C. Brechignac, M. Broyer, Ph. Cahuzac, G. Delacretaz, P. Labasie, and L. Wöste, Chem. Phys. Lett. **120**, 559 (1985); C. Brechignac, M. Broyer, P. Cahuzac, G. Delacretaz, P. Labasie, J. P. Wolf, and L. Wöste, Phys. Rev. Lett. **60**, 275 (1988).
[4] H. Haberland, B. von Issendorff, Y. Yufeng, and T. Kolar, Phys. Rev. Lett. **69**, 3212 (1992); K. Rademann, O. Dimopoulou-Rademann, M. Schlauf, U. Even, and F. Hensel, Phys. Rev. Lett. **69**, 3208 (1992).
[5] B. Kaiser and K. Rademann, Phys. Rev. Lett. **69**, 3204 (1992).
[6] H. Haberland, H. Kornmeier, H. Langosch, M. Oschwald, and G. Tanner, J. Chem. Soc., Faraday Trans. **86**, 2473 (1990).
[7] K. Rademann, B. Kaiser, U. Even, and F. Hensel, Phys. Rev. Lett. **59**, 2319 (1987); K. Rademann, Ber. Bunsenges. Phys. Chem. **93**, 653 (1989).
[8] G. M. Pastor, P. Stampfli, and K. H. Bennemann, Europhys. Lett. **7**, 419 (1988); see also Ref. [2].
[9] R. Busani, M. Folkers, and O. Cheshnovsky, Phys. Rev. Lett. **81**, 3836 (1998).
[10] R. Busani, M. Folkers, and O. Cheshnovsky, Philos. Mag. B **79**, 1427 (1999).
[11] U. Even, J. Jortner, D. Noy, N. Lavie, and C. Cossart-Magos, J. Chem. Phys. **112**, 8068 (2000).
[12] P. Kruit and F. H. Read, J. Phys. E **16**, 313 (1983).
[13] O. Cheshnovsky, S. H. Yang, C. L. Pettiette, M. J. Craycraft, and R. E. Smalley, Rev. Sci. Instrum. **58**, 2131 (1987).
[14] Sunlite OPO system, pumped by 9010 Powerlite Nd/YAG laser, Continuum. Typical laser pulses: 50–300 μJ, 4 mm^2, 5 ns. To ensure spectral purity, light was directed to the system using a Pellin Broca prism.
[15] R. Giniger, T. Hippler, S. Ronen, and O. Cheshnovsky, Rev. Sci. Instrum. **72**, 2543 (2001).
[16] G. Gantefor, W. Eberhardt, H. Weidele, D. Kreisle, and E. Recknagel, Phys. Rev. Lett. **77**, 4524 (1996).
[17] J. C. Pinare, B. Baguenard, C. Bordas, and M. Broyer, Eur. Phys. J. D **9**, 21 (1999); C. Bordas, J. C. Pinare, B. Baguenard, and M. Broyer, J. Phys. IV (France) **10**, 55 (2000).
[18] L. S. Wang, J. Conceicao, C. Jin, and R. E. Smalley, Chem. Phys. Lett. **182**, 5 (1991); J. U. Andersen, C. Brink, P. Hvelplund, M. O. Larsson, B. Bech Nielsen, and H. Shen, Phys. Rev. Lett. **77**, 3991 (1996).
[19] R. Schlipper, R. Kusche, B. von Issendorff, and H. Haberland, Appl. Phys. A **72**, 255 (2001).
[20] N. Pontius, P. S. Bechthold, M. Neeb, and W. Eberhardt, Phys. Rev. Lett. **84**, 1132 (2000).
[21] N. Pontius, P. S. Bechthold, M. Neeb, and W. Eberhardt, Appl. Phys. B **71**, 351 (2000).
[22] For Hg_{20}, BG = 1.8 eV and EA = 2.3 eV; for Hg_{40}, BG = 1.2 eV and EA = 3.0 eV.
[23] G. Bar Chaim, R. Busani, R. Giniger, and O. Cheshnovsky (to be published).
[24] V. I. Klimov, A. A. Mikhailovsky, D. W. McBranch, C. A. Leatherdale, and M. G. Bawendi, Science **287**, 1011 (2000).
[25] S. Minemoto, J. Muller, G. Gantefor, H. J. Munzer, J. Boneberg, and P. Leiderer, Phys. Rev. Lett. **84**, 3554 (2000).